Available online at http://www.ssstj.sci.ssru.ac.th

Suan Sunandha Science and Technology Journal

Structural and Oxidation Behavior of Nanocomposite TiCrN Thin Films

Siriwat Alaksanasuwan[1,3*], Adisorn Buranawong[2,3] and Nirun Witit-anun[2,3]

[1]Faculty of Science and Technology, Phranakhon Si Ayutthaya Rajabhat University, Phranakhon Si Ayutthaya 13000, Thailand
[2]Department of Physics, Faculty of Science, Burapha University, Chonburi 20131, Thailand
[3]Thailand Center of Excellence in Physics (ThEP), MHESI, Bangkok 10400, Thailand
***Corresponding author e-mail: siriwat.aru@gmail.com**

Received: *17 February 2022* /**Revised**: *1 March 2022* / **Accepted:** *26 May 2022*

Abstract

The structural and oxidation behavior of nanocomposite titanium chromium nitride (TiCrN) thin films has been investigated by using x-ray diffraction (XRD), energy dispersive x-ray spectroscopy (EDS), and field emission scanning electron microscopy (FE-SEM). The TiCrN thin films were deposited on Si substrates by using the reactive DC magnetron sputtering technique from the Ti-Cr mosaic target. After that, the as-deposited thin films were annealed in the air at 500 - 900°C for 2 h. The XRD results showed that the formation oxidation of anatase-TiO_2, rutile-TiO_2, and Cr_2O_3 which diffraction peak appear from 500°C. The relative intensity of these oxide peaks varied with the annealed temperatures. By observing from FE-SEM, the aggregation of the grain increased with the annealing temperature. The cross-sectional results showed that the thin dense oxide overlayer occurred at 700°C and the oxide thickness increased gradually with the annealing temperature. Meanwhile, underneath the TiCrN grain grew above 700°C and become more void structure after annealing at 700°C. The dramatically increase of the oxygen content was found at 700°C and the evolution of Ti, Cr, N, and O with different elements compositions at various annealing temperatures were investigated from the EDS technique. The oxide layer obviously grows inward indicating the oxidation of TiCrN thin films belongs to inward oxidation. The oxidation rate of the films was increased with the increase of annealing temperature. The activation energy of the oxidation as evaluated by the Arrhenius-type relation was 168 kJ/mol.

Keywords: TiCrN thin film, Oxidation, Reactive sputtering, Mosaic target

1. Introduction

Nowadays, nano-layer hard coatings are very important in the manufacture of mechanical tools. This is because of high demand and its impact on the industrial part is those for surface hardening of conventional materials, which can be used efficiently to extend the lifetime of these tools (Solis-Pomar et al., 2016). Particularly, nitride coatings are commonly used as hard, wear-resistant, and anti-corrosion coatings because of their excellent properties (Santecchia et al., 2015). TiN was the first PVD ceramic coating used successfully to mechanical tools in the industry and it is still the most recognized (Alberdi, Marin, Diaz, Sanchez, & Galindo, 2007). However, the limitation of TiN is very rapid oxidation at temperatures above 500°C that easily induces shear off of the coating film and contributes to the degradation (Komarov, Konstantinov, Kovalchuk, Konstanttinov, & Tkachenko, 2016). It has been reported that the thermal oxidation resistance of TiN is considerably increased by the addition of chromium (Cr) in the TiN structure which leads to the ternary coating of TiCrN (Choi, Han, Hong, & Lee, 2009; Thampi, Bendavid, & Subramanian, 2016). Owing to the incorporation of Cr atom in the cubic fcc TiN structure influences the structure which leads to increase the hardness of TiN films from 20-25 GPa to 22-35 GPa and extended the oxidation resistance of the TiN films from 500°C to above 700°C (Chang, Yang, & Wang, 2007; Chen, Luo, & Zhao, 2013; Uglov, Anishchik, Zlotski, Abadias, & Dub, 2005; Vishnyakov et al., 2006). Hence, TiCrN coatings have become used as hard coatings for tools recently, in particular for high-speed cutting tools (Uglov et al., 2005).

Commonly, the TiCrN thin films can be prepared by two main PVD methods: evaporation (Chen et al., 2013; Wolfe, Gabriel, & Reedy, 2011) and sputtering (Krzanowski & Foley, 2014;

Suan Sunandha Science and Technology Journal

Paksunchai, Denchitcharoen, Chaiyakun, & Limsuwan 2012). The reactive magnetron sputtering is one of the most widely used methods to prepare thin films with large area uniformity and strong adhesion (Thampi et al., 2016). Moreover, a tactic in evolving the method of magnetron sputtering for depositing multicomponent thin films such as TiCrN films with any content of elements using a single magnetron is the use of a mosaic target (a target that consists of a regular target of Ti with inserts by Cr). Additionally, the sputtering by using a mosaic target may be suitable for deposited hard coatings with low mutual solubility or a great difference in melting temperatures (Alaksanasuwan, Buranawong, & Witit-Anun, 2020; Golosov, Melnikov, & Dostanko, 2012).

It is well known that the properties of thin films strongly depend on the microstructure of films which relates to the deposition parameters such as nitrogen gas flow rate, sputtering current, voltage bias, substrate temperature, partial or total pressure, and other parameters. Therefore, the effect of deposition parameters on the structural and properties of TiCrN thin films is still important. Furthermore, the demand to develop new hard coatings with good thermal stability has become essential to enhance tool life as machining speed increases (Chim, Ding, Zeng, & Zhang, 2009; Rizzo et al., 2013). Most high-temperature coatings depend on the formation of a protective oxide scaled by interaction with the environment (Chim et al., 2009). However, few annealing at high-temperature studies were performed on TiCrN thin film in terms of structure and properties. Therefore, the relation between thin films and their properties under various annealing temperatures is still essential to investigate.

This research work aimed to understand and discuss the structural and oxidation behavior of nanocomposite titanium chromium nitride (TiCrN) thin films deposited by the reactive DC magnetron sputtering using a mosaic target. Phase formation, morphological and elemental composition change during elevated temperature, which annealing the as-deposited thin films at high temperatures ranging from 500 to 900°C in air was investigated.

2. Experimental Details

TiCrN thin films in this research work were deposited on Si (100) substrate by the homemade vacuum coater as shown in Figure 1 with reactive DC magnetron sputtering technique from a mosaic target. The Ti-Cr mosaic target style, used in this research work, is made by embedding chromium rods (99.99%) into the high sputtering rate area of metal titanium (99.97%) disk, with a diameter of 54 mm and thickness of 3 mm thick. Pure Ar (99.999%) and N_2 (99.999%) were used as the sputtering and reactive gasses, respectively. Before deposition, the coating chamber was evacuated to a base pressure of 5×10^{-5} mbar. Previous to the deposition of the process of thin film, the pre-sputtering stage was start-up by ion bombardment from Ar^+ ions, which sputtered on the target to eliminate the surface impurities under a shutter shielding in about 5 min. The TiCrN films were deposited at 60 min, while the deposition parameters such as Ar and N_2 gas flow rate, sputtering power, substrate-target distances, substrate temperature, and working pressure were constant. The deposition parameters are summarized in Table 1.

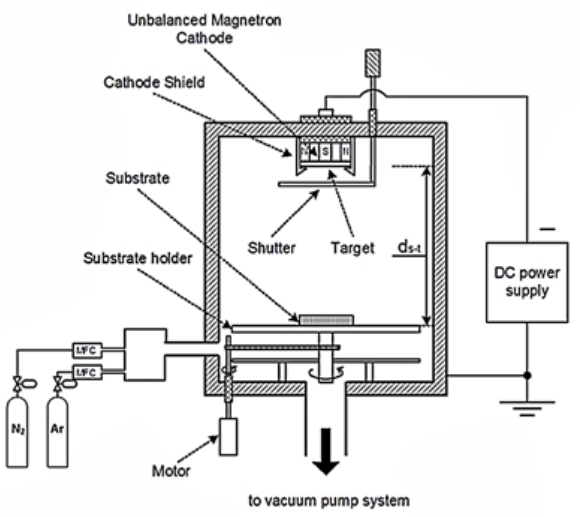

Figure 1. The homemade DC magnetron sputtering coater diagram.

Table 1. Deposition conditions of TiCrN thin films.

Parameters	Value
Sputtering targets	Mosaic of Ti-Cr
Substrate	Si (100)
Ar flow rate	16 sccm
N_2 flow rate	6 sccm
Base pressure	5.0×10^{-5} mbar

Suan Sunandha Science and Technology Journal

Working pressure	5.0×10^{-3} mbar
Sputtering Power	190 W
Target to substrate distance	15 cm
Deposition time	60 min

The crystalline structure of the as-deposited TiCrN thin film was analyzed by grazing-incidence X-ray diffraction (GIXRD: Bruker D8) using monochromatic Cu-k_α as an X-ray source ($\lambda = 0.154$ nm). The XRD patterns were acquired in a continuous mode, the 2θ scan angle range is between 20° and 80° with a measurement step of 0.02° min^{-1} and the grazing incidence angle of 3°. The phase of the film was determined using Bragg's law and interplanar spacing equation and compared with the Joint Committee on Powder Diffraction Standard (JCPDS) files. The microstructure, thickness, and cross-section structure of the thin films were observed by Field Emission Scanning Electron Microscope (FE-SEM: Hitachi s4700). The elemental composition of the TiCrN thin films was measured by energy-dispersive X-ray spectroscopy (EDS: EDAX) which connected to the Scanning Electron Microscope (SEM: LEO 1450VP).

The oxidation behavior of the TiCrN thin films was evaluated by the annealing process which was heated by a furnace (CARBOLITE: CWF1300) at a different temperature ranging from 500 to 900 °C with 100 °C increments for each step under the constant heating time of 2 h in the air atmosphere. After that, the oxidation behavior of thin films was investigated by XRD, FE-SEM, and EDS for identifying the formation of oxide structure, the cross-sectional oxide layer, and O content, respectively. In order to understand the oxidation behavior of the TiCrN films, the oxidation rate in cm^2/s, $k_p(T)$ related to the thickness of oxide layer from cross-sectional observation in cm, d and annealing time in s, t was calculated from Wagner's parabolic oxidation theory (Qi et al., 2013), whereby

$$d = 2[k_p(T) \times t]^{1/2} \qquad (1)$$

The activation energy (E_a) in kJ of the films was obtained from the slope of the linear regression using the Arrhenius equation (Qi et al., 2013), whereby k_{p0} is the pre-exponential factor (cm^2/s), E_a is the activation energy (kJ), R is the gas constant (8.31 $J \cdot K^{-1} \cdot mol^{-1}$) and T is the annealing temperature (K), are calculated from

$$k_p(T) = k_{p0} \exp(-E_a/RT) \qquad (2)$$

3. Results and Discussion

The X-ray diffraction patterns of the TiCrN films prepared on a Si wafer are shown in Figure 2. The lines at 2θ values of standard TiN and CrN with (111), (200), and (220) planes were exhibited for comparison purposes. The results from the XRD technique revealed that the crystal structures of the as-deposited TiCrN thin films prepared on Si wafers were revealed that the 2θ values of diffraction peaks varied between the TiN and CrN JCPDS standard data of 87-0633 and 77-0047, respectively, as shown in Figure 2. Moreover, the diffraction peaks varied between the TiN and CrN JCPDS standard structure. These results were according to the TiCrN (111), (200), and (220) plane.

The solid solution of (Ti,Cr)N film is a composite structure of TiN and CrN that has a similar crystal structure and nearby lattice parameter (Choi et al., 2009). Furthermore, it has been reported that the FCC B1-NaCl phase of the (Ti,Cr)N film was attained by using magnetron sputtering. (Choi et al., 2009; Paksanchai et al., 2012; Thampi et al., 2016). Actually, the solid solution of (Ti,Cr)N was formed whereby the Ti atoms were substituted by Cr atoms in TiN structure due to the atomic radius of Cr (0.1249 nm) is lesser than the radius of the Ti atom (0.1445 nm) (Paksanchai et al., 2012).

Figure 2 shows the XRD patterns of the TiCrN films after annealing, the results revealed that the diffraction angle of oxide structures for TiO_2 and Cr_2O_3 phases were found after annealing at 500°C and 600°C. These structures were in good agreement with the JCPDS standard no.89-4921 tetragonal TiO_2 anatase structure of (004) planes, JCPDS no. 89-4920 tetragonal TiO_2 rutile structure of (210) planes, and JCPDS no. 82-1484 rhombohedral Cr_2O_3 of (214) planes were obtained, respectively. Moreover, it was found that the crystallinity of these oxide structures increased with the increase of annealed temperatures from 500 to 600°C. Then, it was found that the crystal structure of films was changed after annealing at 700°C. The TiO_2 rutile structure of (101) planes were obtained, whereas other oxide phases still appeared, but it was found the dramatically decreased crystallinity of these

Suan Sunandha Science and Technology Journal

oxide phases. Lastly, the significantly increased crystallinity with strongly preferred orientations along TiO_2 (101) was noticed for the annealing temperature reaching 800℃. Additionally, the rhombohedral Cr_2O_3 phase of (113) appeared.

It could be attributed to the O_2 from the annealing atmosphere that reacted with the TiCrN thin films which resulted in forming the TiO_2 and Cr_2O_3 by oxidation mechanism (Chen & Lu, 2006). The crystallinity enhancement observed from X-ray intensity increased may be due to the aggregation deposited atom resulting in more order atom arrangement and the reduction of the defect during the annealing temperatures (Wang et al., 2013). Additionally, it was found that solid solution TiCrN thin film was changed to oxide structure of TiO_2 and Cr_2O_3 phases at annealed above 500°C from XRD analysis. Therefore, the TiCrN films in this work can resist thermal oxidation at 500°C.

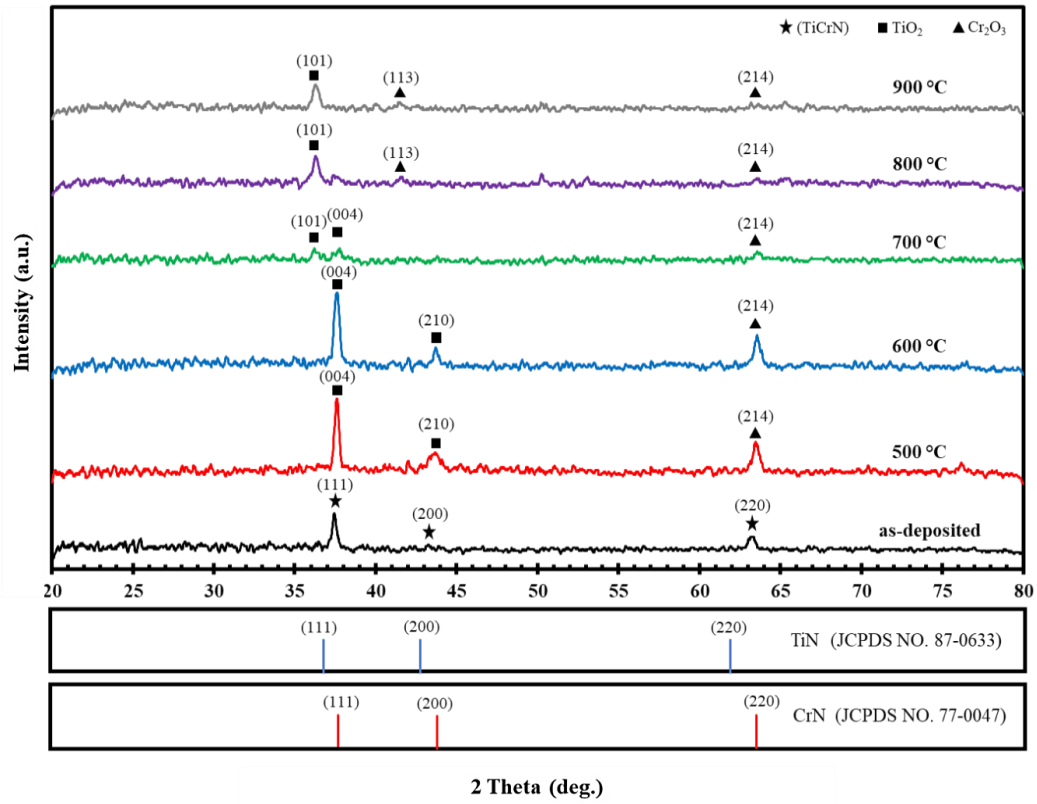

Figure 2. X-ray diffraction patterns of the TiCrN thin film before and after annealing.

The EDS result shows the as-deposited thin film and annealed thin film's chemical composition as a function of the annealing temperature in the air environment (Table 2 and Figure 3). As the annealing temperature below 600℃, the TiCrN thin films contained the Ti, Cr, N, and O composition of about 9, 21, 40, and 30 at.%, respectively. As the annealing temperature elevated above 700℃, it was found that the N content in the films was dramatically decreased from about 40 to 10 at.%, whereas a complete addition of the O contents in the films from about 30 to 60 at.%. Meanwhile, the Ti and Cr contents were still in the range of 7.38 to 7.51 at.% and 17.23 to 18.26 at.%, respectively.

It could be concluded that the elemental composition analysis results are in good agreement with the findings of the crystal structure characterization. It suggested that the thin films annealed at over 700℃ changed the structure of film with phase segregation owing to the heating process. The continuous increase of O contents after annealing is because the O_2 from the ambient atmosphere was diffused into the film and replaced as the N atoms in TiCrN films resulting from the dramatically decrease of N content by the oxidation mechanism during annealing temperature (Aliaj, Syla, Oettel, & Dilo, 2016). Consequently, the increase of O content from the EDS technique can

Suan Sunandha Science and Technology Journal

obviously be confirmed that the thin film oxidation occurred.

Table 2. The compositions and thickness of the TiCrN thin films at different annealing temperatures.

Annealing temperature (°C)	Thin film thickness (nm)	Compositions (at.%)			
		Ti	Cr	N	O
As-deposited	532	8.77	21.00	40.36	29.87
500	534	8.72	20.64	40.20	30.44
600	540	8.69	20.80	39.94	30.56
700	556	7.38	17.23	25.90	49.49
800	665	7.36	17.64	16.93	58.07
900	627	7.51	18.26	10.74	63.49

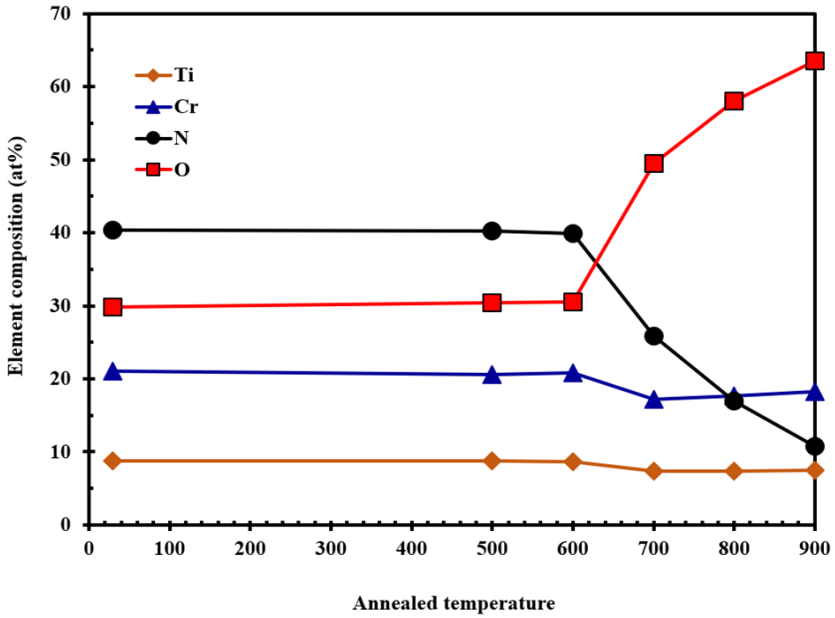

Figure 3. The element compositions of TiCrN thin films as a function of as-deposited to annealing temperatures.

The microstructure and the cross-sectional of the TiCrN thin films after the annealing process in the range of 500 to 900°C for 2 hours in the air were observed by the FE-SEM technique as shown in Figure 4 and 5. Firstly, Figure 4 exposes the films after the annealing process. Small grains and smooth surfaces were also found over the surface of the as-deposited films (Figure 4a). As the annealing temperature at 500 and 600°C, it can be seen that the surface pattern was stilled unchanged from the as-deposited films (Figure 4b and 4c). Thus, the TiCrN thin films in this work were also shown the thermal oxidation resistance up at 600°C. As the annealing temperature increased up to 700°C, it was found that countless grains with different shapes and sizes with a void between the grain boundaries were observed (Figure 4d). Grain aggregation, more void, and increased their sizes were identified when the annealing temperature reached 800°C (Figure 4e). Lastly, the surface of films at the highest annealing temperature of 900°C revealed that the grains are found to be continuous (Figure 4f).

The changing of grain sizes resulting from the increasing of the annealing temperature was investigated. The grain sizes growing with increasing of the annealing temperature may be controlled by a mechanism that the energy additional provided by higher annealing temperature formerly increases the mobility of deposited atoms resulting in grain coalescence (Mayrhofer, Willmann, & Mitterer, 2001). Additionally, it could be explained by considering the annealing induced

Suan Sunandha Science and Technology Journal

coalescence of small grains by grain boundary diffusion which resulted in major grain growth (Jafari et al., 2014).

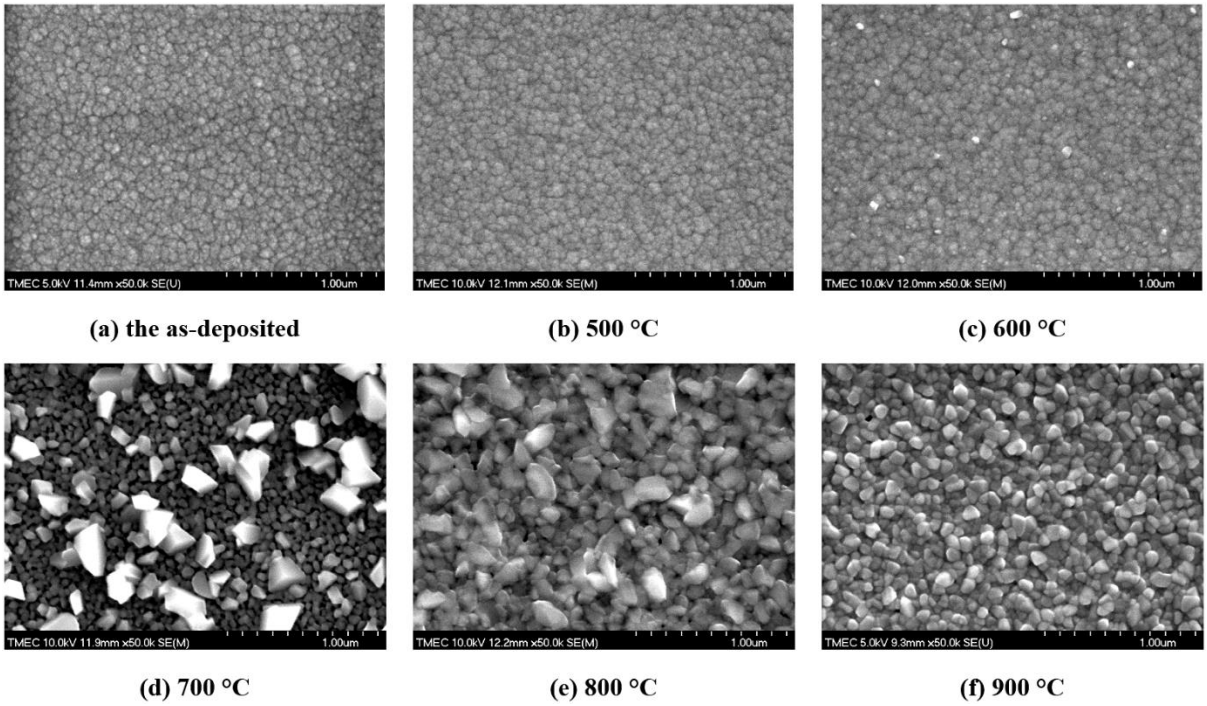

Figure 4. FE-SEM micrographs of TiCrN thin films annealed at different temperatures.

Figure 5 presents the FE-SEM images of the cross-section of TiCrN films after the annealing process. The microstructure of the as-deposited TiCrN thin films consists of columnar growth due to the nearly equiaxed grains stacked one upon other such that grain size is similar to the column diameter (Figure 5a). After annealing at high temperature, it was found that the cross-section observation apparently reveals the film also performs a columnar pattern as the annealing temperature at 500 to 600°C (Figure 5b and 5c). A non-columnar formation can be observed and appear as a facet grain with a void at over 700°C (Figure 5d). At an annealing temperature up to 800°C, grains combine forming a polygon shape structure and increasing their void between grains (Figure 5e). Finally, for annealed at 900°C showed less voided but significant in grain coalescence (Figure 5f).

It can be confirmed that the TiCrN thin films in this research work were also shown the thermal oxidation resistance at 500°C. At a higher temperature of above 700°C, the cross-section structure of the TiCrN thin films was changed to an oxide structure owing to the thermal oxidation process. Moreover, it is clearly seen that after annealing, the cross-sectional transformation can be seen due to the higher annealing temperature, the grain mobility increases, and more the coalescence of the grain. Hence, the FE-SEM results in this work can visibly confirm that the annealing temperature can be influenced by the cross-sectional morphology of the films.

Suan Sunandha Science and Technology Journal

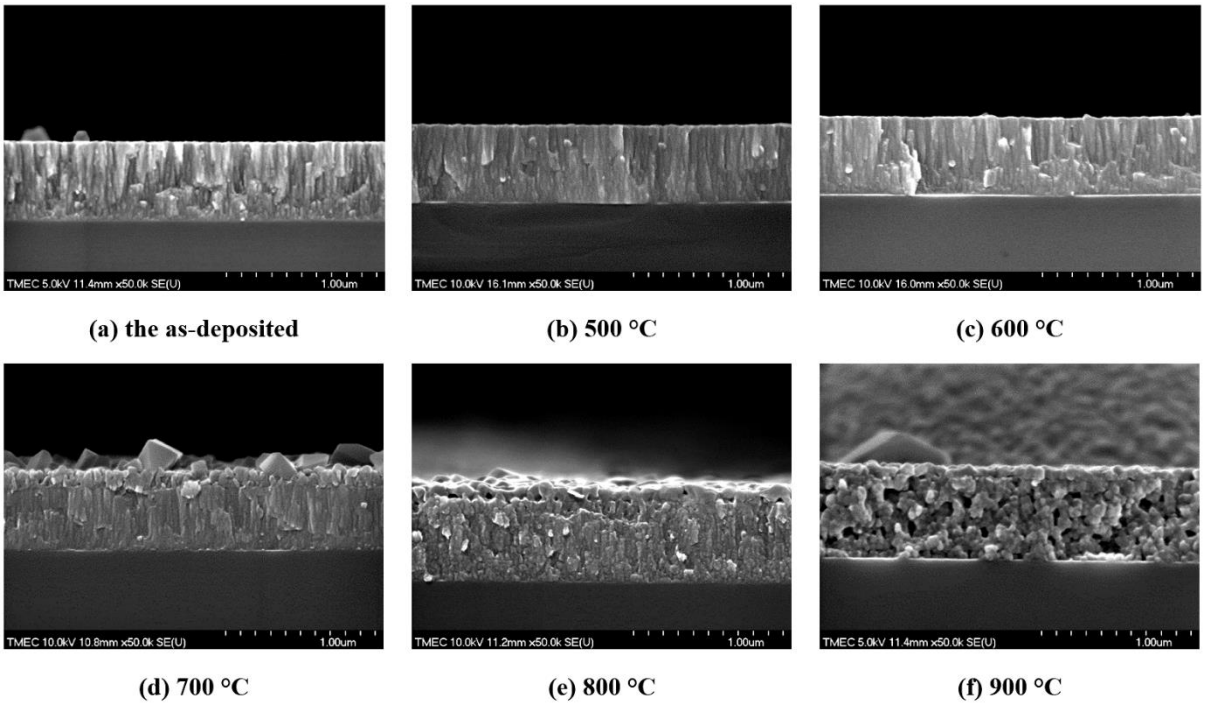

Figure 5 FE-SEM cross-section of TiCrN thin films annealed at different temperatures.

The oxidation rate, $k_p(T)$ at a given oxidation temperature of TiCrN thin film was obtained from the parabolic relation as shown in Table 3. It was revealed that the increase of oxidation rate from 4.05×10^{-15} to 1.36×10^{-13} cm^2/s as the annealing temperature increased from 700 to 900ºC. The activation energy (E_a) is evaluated from the Arrhenius equation. The Arrhenius plot of $\ln[k_p(T)]$ as a function of 1/1000 T for oxidized TiCrN thin film was shown in Figure 6. In this work, the activation energy of TiCrN thin film was calculated as 168 kJ/mol. It was found that the activation energy of TiCrN thin films in this study was different from other works. Otani and Hofmann have reported the activation energy of TiCrN films were the range of 120-140 kJ of annealing temperature ranging from 400 to 700°C for 10 and 300 min in the air (Otani & Hofmann, 1996). Nevertheless, the TiCrN films in their work were prepared by reactive magnetron co-sputtering technique at varied Ti/Cr ratios and the thickness of films was controlled at 2-3 µm. Therefore, the oxidation behavior may be depending on the stoichiometry or thickness of films.

Table 3. The film thickness, oxide thickness, and oxidation rate of the TiCrN thin films and after annealing in the air for 2 h at various temperatures ranging from 500 to 900°C.

Annealing Temperature (ºC)	Film thickness (nm)	Oxide thickness (nm)	Oxidation rate (cm^2/s)
As-deposited	532	-	-
500	534	-	-
600	540	-	-
700	556	108	4.05×10^{-15}
800	665	345	4.13×10^{-14}
900	627	627	1.36×10^{-13}

Suan Sunandha Science and Technology Journal

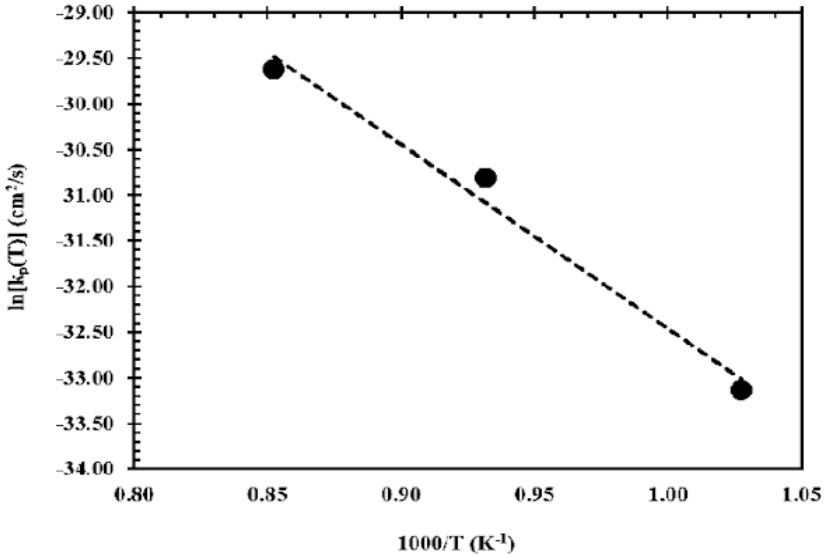

Figure 6. The Arrhenius plot of the TiCrN thin films oxidized at various annealing temperatures.

4. Conclusion

The structural and oxidation behavior of nanocomposite titanium chromium nitride (TiCrN) thin films, deposited on Si substrates by using the reactive DC magnetron sputtering technique from the mosaic target, was characterized between 500 and 900ºC in the air using XRD, EDS, and FE-EM techniques. It was found that the annealing temperature strongly influences the structure of the thin films. The transformation of polycrystalline TiCrN to TiO_2 and Cr_2O_3 structure, in which the relative intensity of these oxide peaks varied with the annealed temperatures, were obtained from XRD patterns. The changing of grains has resulted from the increase of annealing temperature as investigated from the FE-SEM. The cross-sectional results showed that the thin dense oxide layer occurred at 700°C and the oxide thickness increased gradually with the annealed temperature. Meanwhile, underneath the TiCrN grain grew above 700°C and become more void structure after annealing at 700°C. The oxide layer obviously grows inward indicating the oxidation of TiCrN thin films belongs to inward oxidation. The EDS result was also in good agreement with the XRD technique that the crystal structure, of the TiCrN films, changed which significantly increased of the O content but rapidly decreased and was constant of the Ti, Cr, and N contents when annealed the films from 700°C. The oxidation rate of the films was increasing from 4.05×10^{-15} to 1.36×10^{-13} cm^2/s with the increase of annealing temperature. The activation energy of the oxidation as evaluated by the Arrhenius-type relation was 168 kJ/mol.

5. References

Alaksanasuwan, S., Buranawong, A., & Witit-Anun, N. (2020). Effect of sputtering current on the structure of TiCrN thin films prepared from mosaic target by reactive DC magnetron sputtering. *Applied Mechanics and Materials*, *901*, 37-42. doi:10.4028/www.scientific.net/AMM.901.37

Alberdi, A., Marin, M., Diaz, B., Sanchez, O., & Galindo, R. E. (2007). Wear resistance of titanium-aluminium-chromium-nitride nanocomposite thin films. *Vacuum*, *81*, 1453-1456. doi:10.1016/j.vacuum.2007.04.024

Aliaj, F., Syla, N., Oettel, H., & Dilo, T. (2016). Thermal treatment in air of direct current (DC) magnetron sputtered TiN coatings. *Scientific Research and Essays*, *11*(21), 230-238. doi:10.5897/SRE2016.6456

Chang, Y.-Y., Yang, S.-J., & Wang, D.-Y. (2007). Characterization of TiCr(C,N)/amorphous carbon coatings synthesized by a cathodic arc deposition process. *Thin Solid Films*, *515*, 4722-4726. doi:10.1016/j.tsf.2006.11.028

Chen, H. Y., & Lu, F. H. (2006). Oxidation behavior of chromium nitride films. *Thin Solid Films*, *515*, 2179-2184. doi:10.1016/j.tsf.2006.06.039

Suan Sunandha Science and Technology Journal

Chen, S., Luo, D., & Zhao, G. (2013). Investigation of the properties of $Ti_xCr_{1-x}N$ coatings prepared by cathodic arc deposition. *Physics Procedia*, *50*, 163-168. doi:10.1016/j.phpro.2013.11.027

Chim, Y. C., Ding X. Z., Zeng, X. T., & Zhang, S. (2009). Oxidation resistance of TiN, CrN, TiAlN and CrAlN coatings deposited by lateral rotating cathode arc. *Thin Solid Films*, *517*, 4845-4849. doi:10.1016/j.tsf.2009.03.038

Choi, H. S., Han, D. H., Hong, W. H., & Lee, J. J. (2009). (Titanium, chromium) nitride coatings for bipolar plate of polymer electrolyte membrane fuel cell. *Journal of Power Sources*, *189*, 966-971. doi:10.1016/j.jpowsour.2008.12.060

Golosov, D. A., Melnikov, S. N., & Dostanko, A. P. (2012). Calculation of the elemental composition of thin films deposited by magnetron sputtering of mosaic targets. *Surface Engineering and Applied Electrochemistry*, *48*, 52-59. doi:10.3103/S1068375512010073

Jafari, A., Ghoranneviss, Z., Solar Elahi, A., Ghoranneviss, M., Fasihi Yazdi, N., & Rezaei, A. (2014). Effects of annealing on TiN thin film growth by DC magnetron sputtering. *Advances in Mechanical Engineering*, *2014*, 1-6. doi:10.1155/2014/373847

Komarov, F. F., Konstantinov, V. M., Kovalchuk, A. V., Konstantinov S. V., & Tkachenko, H. A. (2016). The effect of steel substrate pre-hardening on structural, mechanical, and tribological properties of magnetron sputtered TiN and TiAlN coating. *Wear*, *352-353*, 92-101. doi:10.1016/j.wear.2016.02.007

Krzanowski, J. E., & Foley, D. J. (2014). The effect of Cr content on the oxidation behavior of Ti-Cr-N films. *Coatings*, *4*, 308-319. doi:10.3390/coatings4020308

Mayrhofer, P. H., Willmann, H., & Mitterer, C. (2001). Oxidation kinetics of sputtered Cr-N hard coatings. *Surface and Coatings Technology*, *146-147*, 222-228. doi:10.1016/s0257-8972(01)01471-2

Otani, Y., & Hofmann, S. (1996). High temperature oxidation behaviour of $(Ti_{1-x}Cr_x)N$ coatings. *Thin Solid Films*, *287*, 188-192. doi:10.1016/s0040-6090(96)08789-5

Paksunchai, C., Denchitcharoen, S., Chaiyakun, S., & Limsuwan, P. (2012). Effect of sputtering current on structure and morphology of $(Ti_{1-x}Cr_x)N$ thin films deposited by reactive unbalanced magnetron co-sputtering. *Procedia Engineering*, *32*, 875-881. doi:10.1016/j.proeng.2012.02.026

Qi, Z. B., Liu, B., Wu, Z. T., Zhu, F. P., Wang, Z. C., & Wu, C. H. (2013). A comparative study of the oxidation behavior of Cr_2N and CrN coatings. *Thin Solid Films*, *544*, 515-520. doi:10.1016/j.tsf.2013.01.031

Rizzo A., Mirenghi, L., Massaro, M., Galietti, U., Capodieci, L., Terzi, R., … Valerini, D. (2013). Improved properties of TiAlN coatings through the multilayer structure. *Surface and Coatings Technology*, *235*, 475-483. doi:10.1016/j.surfcoat.2013.08.006

Santecchia, E., Hamouda, A. M. S., Musharavati, F., Zalnezhad, E., Cabibbo, M., & Spigarelli, S. (2015). Wear resistance investigation of titanium nitride-based coatings. *Ceramics International*, *41*, 10349-10379. doi:10.1016/j.ceramint.2015.04.152

Solis-Pomar, F., Nápoles, O., Vázquez Robaina, O., Gutierrez-Lazos, C., Fundora, A., Colin, A., … Melendrez, M. F. (2016). Preparation and characterization of nanostructured titanium nitride thin films at room temperature. *Ceramics International*, *42(6)*, 7571-7575. doi:10.1016/j.ceramint.2016.01.164

Thampi, V. V. A., Bendavid, A., & Subramanian, B. (2016). Nanostructured TiCrN thin films by pulsed magnetron sputtering for cutting tool applications. *Ceramics International*, *42*, 9940-9948. doi:10.1016/j.ceramint.2016.03.095

Uglov, V. V., Anishchik, V. M., Zlotski, S. V., Abadias, G., & Dub, S. N. (2005). Stress and mechanical properties of Ti-Cr-N gradient coatings deposited by vacuum arc. *Surface and Coatings Technology*, *200*, 178-181. doi:10.1016/j.surfcoat.2005.02.136

Vishnyakov, V. M., Bachurin, V. I., Minnebaev, K. F., Valizadeh, R., Teer, D. G., Colligon, J. S., … Yurasova, V. E. (2006). Ion assisted deposition of titanium chromium nitride. *Thin Solid Films*, *497*, 189-195. doi:10.1016/j.tsf.2005.05.005

Suan Sunandha Science and Technology Journal

Wang, F., Wu, M. Z., Wang, Y. Y., Yu, Y. M., Wu, X. M., & Zhuge, L. J. (2013). Influence of thickness and annealing temperature on the electrical, optical and structural properties of AZO thin films. *Vacuum*, *89*, 127-131. doi:10.1016/j.vacuum.2012.02.040

Wolfe, D. E., Gabriel, B. M., & Reedy, M. W. (2011). Nanolayer (Ti,Cr)N coatings for hard particle erosion resistance. *Surface and Coatings Technology*, *205*, 4569-4576. doi:10.1016/j.surfcoat.2011.03.121